Three-dimensional temperature distribution and modification mechanism in glass during ultrafast laser irradiation at high repetition rates

AUTHOR(S):

Shimizu, Masahiro; Sakakura, Masaaki; Ohnishi, Masatoshi; Yamaji, Masahiro; Shimotsuma, Yasuhiko; Hirao, Kazuyuki; Miura, Kiyotaka

CITATION:

Shimizu, Masahiro ...[et al]. Three-dimensional temperature distribution and modification mechanism in glass during ultrafast laser irradiation at high repetition rates. Optics Express 2012, 20(2): 934-940

ISSUE DATE:

2012-01-16

URL:

http://hdl.handle.net/2433/194089

Three-dimensional temperature distribution and modification mechanism in glass during ultrafast laser irradiation at high repetition rates

Masahiro Shimizu,[1] Masaaki Sakakura,[2,*] Masatoshi Ohnishi,[3] Masahiro Yamaji,[1] Yasuhiko Shimotsuma,[1] Kazuyuki Hirao,[1] and Kiyotaka Miura[1]

[1]*Department of Material Chemistry, Graduate School of Engineering, Kyoto University, Kyoto 615-8510, Japan*
[2]*Center for the Promotion of Interdisciplinary Education and Research, Kyoto University, Kyoto, 606-8501, Japan*
[3]*Futaku Precision Machinery Industry Company, 33-3 Karahashi-Keiden-cho, Minami-ku, Kyoto-shi, Kyoto, 601-8454, Japan*
[*]*msakakura@saci.kyoto-u.ac.jp*

Abstract: We experimentally determined the three-dimensional temperature distribution and modification mechanism in a soda-lime-silicate glass under irradiation of ultrafast laser pulses at high repetition rates by analyzing the relationship between the morphology of the modification and ambient temperature. In contrast to previous studies, we consider the temperature dependence of thermophysical properties and the nonlinear effect on the absorbed energy distribution along the beam propagation axis in carrying out analyses. The optical absorptivity evaluated with the temperature distribution is approximately 80% and at most 3.5% smaller than that evaluated by the transmission loss measurement. The temperature distribution and the strain distribution indicate that visco-elastic deformation and material flow play important roles in the laser-induced modification inside a glass.

OCIS codes: (140.3390) Laser materials processing; (140.3440) Laser-induced breakdown; (140.7090) Ultrafast lasers; (160.2750) Glass and other amorphous materials; (190.4180) Multiphoton processes; (190.4870) Photothermal effects.

References and links

1. A. Vogel, J. Noack, G. Huttman, and G. Paltauf, "Mechanisms of femtosecond laser nanosurgery of cells and tissues," Appl. Phys. B **81**(8), 1015–1047 (2005).
2. S. M. Eaton, H. B. Zhang, P. R. Herman, F. Yoshino, L. Shah, J. Bovatsek, and A. Arai, "Heat accumulation effects in femtosecond laser-written waveguides with variable repetition rate," Opt. Express **13**(12), 4708–4716 (2005).
3. S. M. Eaton, H. Zhang, M. L. Ng, J. Z. Li, W. J. Chen, S. Ho, and P. R. Herman, "Transition from thermal diffusion to heat accumulation in high repetition rate femtosecond laser writing of buried optical waveguides," Opt. Express **16**(13), 9443–9458 (2008).
4. I. Miyamoto, K. Cvecek, and M. Schmidt, "Evaluation of nonlinear absorptivity in internal modification of bulk glass by ultrashort laser pulses," Opt. Express **19**(11), 10714–10727 (2011).
5. S. Kanehira, K. Miura, and K. Hirao, "Ion exchange in glass using femtosecond laser irradiation," Appl. Phys. Lett. **93**(2), 023112 (2008).
6. S. F. Zhou, N. Jiang, K. Miura, S. Tanabe, M. Shimizu, M. Sakakura, Y. Shimotsuma, M. Nishi, J. R. Qiu, and K. Hirao, "Simultaneous tailoring of phase evolution and dopant distribution in the glassy phase for controllable luminescence," J. Am. Chem. Soc. **132**(50), 17945–17952 (2010).
7. M. Shimizu, K. Miura, M. Sakakura, M. Nishi, Y. Shimotsuma, S. Kanehira, T. Nakaya, and K. Hirao, "Space-selective phase separation inside a glass by controlling compositional distribution with femtosecond-laser irradiation," Appl. Phys., A Mater. Sci. Process. **100**(4), 1001–1005 (2010).
8. A. K. Varshneya, *Fundamentals of Inorganic Glasses* (Academic, 1993).
9. M. Sakakura, M. Shimizu, Y. Shimotsuma, K. Miura, and K. Hirao, "Temperature distribution and modification mechanism inside glass with heat accumulation during 250 kHz irradiation of femtosecond laser pulses," Appl. Phys. Lett. **93**(23), 231112 (2008).
10. M. Shimizu, M. Sakakura, M. Ohnishi, Y. Shimotsuma, T. Nakaya, K. Miura, and K. Hirao, "Mechanism of heat-modification inside a glass after irradiation with high-repetition rate femtosecond laser pulses," J. Appl. Phys. **108**(7), 073533 (2010).

#157072 - $15.00 USD
Received 26 Oct 2011; accepted 15 Nov 2011; published 4 Jan 2012

11. A. Mermillod-Blondin, I. M. Burakov, Y. P. Meshcheryakov, N. M. Bulgakova, E. Audouard, A. Rosenfeld, A. Husakou, I. V. Hertel, and R. Stoian, "Flipping the sign of refractive index changes in ultrafast and temporally shaped laser-irradiated borosilicate crown optical glass at high repetition rates," Phys. Rev. B **77**(10), 104205 (2008).
12. C. B. Schaffer, J. F. Garcia, and E. Mazur, "Bulk heating of transparent materials using a high-repetition-rate femtosecond laser," Appl. Phys., A Mater. Sci. Process. **76**(3), 351–354 (2003).
13. A. Royon, Y. Petit, G. Papon, M. Richardson, and L. Canioni, "Femtosecond laser induced photochemistry in materials tailored with photosensitive agents," Opt. Mater. Express **1**(5), 866–882 (2011).
14. Glass data sheet from Schott.
15. M. Shimizu, M. Sakakura, S. Kanehira, M. Nishi, Y. Shimotsuma, K. Hirao, and K. Miura, "Formation mechanism of element distribution in glass under femtosecond laser irradiation," Opt. Lett. **36**(11), 2161–2163 (2011).
16. H. Mehling, G. Hautzinger, O. Nilsson, J. Fricke, R. Hofmann, and O. Hahn, "Thermal diffusivity of semitransparent materials determined by the laser-flash method applying a new analytical model," Int. J. Thermophys. **19**(3), 941–949 (1998).
17. H. Ohta, H. Shibata, A. Suzuki, and Y. Waseda, "Novel laser flash technique to measure thermal effusivity of highly viscous liquids at high temperature," Rev. Sci. Instrum. **72**(3), 1899–1903 (2001).
18. J. Huang and P. K. Gupta, "Temperature-dependence of the isostructural heat-capacity of a soda lime silicate glass," J. Non-Cryst Sol. **139**, 239–247 (1992).
19. H. Shibata, A. Suzuki, and H. Ohta, "Measurement of thermal transport properties for molten silicate glasses at high temperatures by means of a novel laser flash technique," Mater. Trans. **46**(8), 1877–1881 (2005).
20. K. I. Popov, C. McElcheran, K. Briggs, S. Mack, and L. Ramunno, "Morphology of femtosecond laser modification of bulk dielectrics," Opt. Express **19**(1), 271–282 (2011).
21. M. Shribak and R. Oldenbourg, "Techniques for fast and sensitive measurements of two-dimensional birefringence distributions," Appl. Opt. **42**(16), 3009–3017 (2003).

1. Introduction

When an ultrafast laser pulse is tightly focused inside transparent materials, the light energy is absorbed by the electrons around the focal volume through multiphoton and inverse bremsstrahlung absorption processes. The energy of the photoexcited electrons is transferred to the lattice, and the temperature around the focal volume is elevated [1]. In particular, at high repetition rates (>100 kHz), the thermal energy from each irradiation accumulates around the focal spot because the irradiation rate is faster than that in thermal diffusion, and the characteristic shape modification called "heat modification" occurs by thermal energy [2]. Heat modification has been applied to the fabrication of low-loss optical waveguides [3], laser welding [4], and space-selective control of the material properties of a glass [5–7]. For these applications, the three-dimensional temperature distribution during laser irradiation is important because it can affect the main factors of modification such as stress, material flow, crystallization, and glass transition [8]. Several researchers have investigated the temperature distribution and mechanism of heat modification during high-repetition-rate irradiation [2–4, 9–12]. However, in their analyses, the temperature dependence of thermophysical properties and the nonlinear effect on the absorbed energy distribution along the beam propagation axis have not been considered [13]. In this study, we take these factors into account to determine the three-dimensional temperature distribution and discuss the modification mechanism.

2. Experimental method

We used amplified femtosecond (fs) laser pulses (250 kHz, 70 fs, 800 nm) of a mode-locked Ti-sapphire laser oscillator (Coherent; Mira and RegA). The fs laser pulses were attenuated by a neutral density filter and focused inside a soda-lime-silicate glass plate (Schott B 270 Superwite) [14] with a 20× objective lens (NA = 0.40; Nikon LU Plan ELWD 20). The glass plate was placed on a temperature-controllable stage (Yonekura; MS-TPS), in which the ambient temperature (T_a) could be controlled by infrared radiation from a halogen lamp. The ambient temperature was measured with a thermocouple, which was calibrated by observing the fusions of several metals. Under controlled ambient temperature, the sample was irradiated with fs laser pulses at different pulse energies (1.0, 1.5, and 2.0 μJ) for 1 s.

3. Experimental results

Figures 1(a)–(c) show the optical microscope images of the modified regions after irradiation of 2.0-μJ pulses. Two boundaries are observed in the images [2–4,9,10,15]. In this letter, the

#157072 - $15.00 USD Received 26 Oct 2011; accepted 15 Nov 2011; published 4 Jan 2012

region inside the inner boundary is referred as the "inner-modified region" and that between the inner and outer boundaries is referred as the "outer-modified region." The volume of the outer boundary is larger at higher ambient temperatures. As shown in Figs. 1(d)–(f), the ambient temperature-dependent volume of the outer-modified region can be understood by assuming that the modification occurs above the characteristic temperature threshold (T_{out}). We quantify the size of the outer-modified region by employing R_r and R_z, which are defined in Fig. 1(a). Figure 1(g) shows the ambient temperature dependence of R_r and R_z.

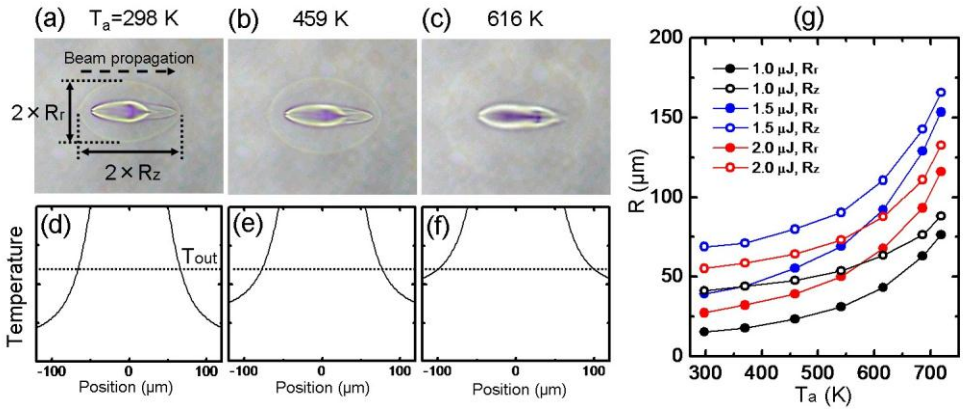

Fig. 1. (a)–(c) Optical microscope images of the modifications induced at various ambient temperatures T_a. The broken arrow indicates the propagation direction of the excitation laser beam. (d)–(f) Schematic explanation of the size change of the outer boundary. T_{out} is the temperature threshold of the modification. (g) Ambient temperature dependences of R_r and R_z at various excitation pulse energies.

4. Analysis

We simulated the thermal energy distribution during laser irradiation to obtain the temperature distribution. The starting equation is Fourier's law:

$$\mathbf{J}(t,\mathbf{r}) = -\lambda\left(T(t,\mathbf{r})\right)\nabla T(t,\mathbf{r}), \tag{1}$$

where $\mathbf{J}(t,\mathbf{r})$ is the flux of thermal energy, λ(T) is the thermal conductivity, $T(t,\mathbf{r})$ is the temperature, ∇ is nabla, t is the time after photoexcitation by the first pulse, and $\mathbf{r}$ is the position vector in Cartesian coordinates. From the definition of specific heat,

$$q(t,\mathbf{r}) = \rho\int_{T_a}^{T(t,\mathbf{r})} C_p(T)dT, \tag{2}$$

where $q(t,\mathbf{r})$ is the thermal energy per unit volume, ρ is the density (weight per unit volume), $C_p(T)$ is the specific heat under constant pressure, and T_a is the ambient temperature. By the equation of continuity, Eqs. (1) and (2), and the heat source by laser irradiation, we obtain the following equation:

$$\frac{\partial q(t,\mathbf{r})}{\partial t} = \nabla\left(D\nabla q(t,\mathbf{r})\right) + \frac{\partial q_{laser}(t,\mathbf{r})}{\partial t}, \tag{3}$$

where $D = \lambda(T(t,\mathbf{r})) / (\rho C_p(T(t,\mathbf{r}))$, which corresponds to the thermal diffusivity. In the first step of the analysis, we assumed the heat source for the single pulse to be expressed as follows [10]:

$$\frac{\partial q_{laser}(t,\mathbf{r})}{\partial t} = \delta\left(t - n\Delta t_L\right) q_0 \exp\left[-\frac{r^2}{(w_r/2)} - \frac{z^2}{(l_z/2)}\right], \tag{4}$$

#157072 - $15.00 USD
Received 26 Oct 2011; accepted 15 Nov 2011; published 4 Jan 2012

where n is the pulse number, Δt_L is the pulse interval (= 4 μs), q_0 is the maximum absorbed energy, $r = (x^2 + y^2)^{1/2}$ is the radial distance, z is the position along the beam propagation axis, and w_r and l_z are the width of absorbed energy in the radial direction (= 1.1 μm, which is determined by the diffraction limit) and that in the beam propagation direction, respectively [Fig. 2(a)]. We used the room-temperature value (4.6×10^{-7} m^2/s) [14] of D for all temperature ranges because there are experimental reports indicating that the change of D is small from 300 K to 1650 K in soda-lime-silicate glasses [16,17]. By using the initial condition of Eq. (4), we can solve Eq. (3) analytically and obtain the time evolution of the energy distribution for one pulse:

$$\Delta q_1(t', \mathbf{r}) = q_0 \frac{(w_r/2)^2}{(w_r/2)^2 + 4Dt'} \cdot \left[\frac{(l_z/2)^2}{(l_z/2)^2 + 4Dt'} \right]^{1/2} \exp\left[-\frac{r^2}{(w_r/2)^2 + 4Dt'} - \frac{z^2}{(l_z/2)^2 + 4Dt'} \right], \quad (5)$$

where t' is the time after the photoexcitation of a certain pulse. After irradiation with the N_{th} pulse, the thermal energy distribution is expressed by

$$q_N(t, \mathbf{r}) = \sum_{n=0}^{N-1} \Delta q_1(t - n\Delta t_L, \mathbf{r}), \quad (6)$$

where n is an integer. The thermal energy distribution can be transformed to a temperature distribution by Eq. (2). We used the temperature dependence of the specific heat shown in Fig. 2(b), which is obtained by shifting the temperature axis in the reported data on soda-lime-silicate glass to match T_g [18]. We did not consider the temperature dependence of the density and used the room-temperature value (2.55×10^3 kg/m^3) [14], because the change of the density is small from 1050 K to 1650 K in a soda-lime-silicate glass [19]. Therefore, the only temperature-dependent material parameter considered in this study is the specific heat. Given our assumption that the temperature at the outer boundary reaches the characteristic temperature T_{out} during laser irradiation, the following relation is obtained at the outer boundary $\mathbf{r} = \mathbf{r}_{boundary}$:

$$q_N(t_{ex}, \mathbf{r}_{boundary}) = \int_{T_a}^{T_{out}} C_p(T) dT, \quad (7)$$

where t_{ex} is the exposure time of the 250-kHz laser pulses (= 1 s). When $\mathbf{r} = (R_r, 0, 0)$ {or $\mathbf{r} = (0, 0, R_z)$} is substituted into Eq. (7), R_r (or R_z) as a function of T_a can be obtained. By fitting the relationship between R_r (or R_z) and T_a by the Eq. (7), q_0, l_z, and T_{out}, can be determined.

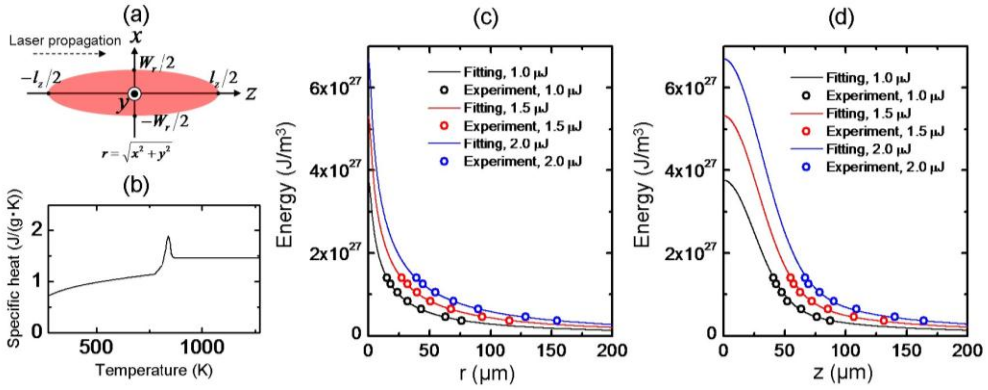

Fig. 2. (a) Heat source in Cartesian coordinates. (b) Specific heat for the simulation. (c) Fitted results for the radial direction. (d) Fitted results for the beam propagation direction. The curves in (c) and (d) are the thermal energy distribution under room temperature irradiation, which were calculated by Eq. (6) with the determined fitting parameter. The plots show the experimental data corresponding to the right-hand side of Eq. (7) with T_{out} determined.

#157072 - $15.00 USD
Received 26 Oct 2011; accepted 15 Nov 2011; published 4 Jan 2012

5. Discussion

We summarize the best-fitting parameters in Table 1 and show the energy distribution curves in Figs. 2(c) and (d). The open circles in Figs. 2(c) and (d) are the thermal energies after 1-s laser irradiation at the positions of $\mathbf{r} = (R_r, 0, 0)$ {or $\mathbf{r} = (0, 0, R_z)$}, which were calculated by the right-hand side of Eq. (7) with T_a and determined T_{out}.

Table 1. Parameters Determined by Fitting R_z, R_r vs. T_a by Eq. (7)[a]

	1.0 μJ	1.5 μJ	2.0 μJ
q_0 (J/m^3)	1.34×10^{28}	1.84×10^{28}	2.25×10^{28}
l_z (μm)	65.0	72.8	80.8
T_{out} (K)	834	831	831

[a]The fitting was conducted by minimizing the mean squared error.

The thermal energy (Q_a) due to single photoexcitation can be obtained by integrating Eq. (7) over all space:

$$Q_a = \pi^{3/2} q_0 (w_r / 2)^2 (l_z / 2). \quad (8)$$

The optical absorptivities calculated by dividing Q_a by the pulse energy are shown in Fig. 3(a). As the reference, we also show the absorptivity determined by the transmission loss measurement [shown in the inset of Fig. 3(a)]. The optical absorptivity determined by Q_a corresponds to the lower limit of absorptivity because the absorbed light energy should not include photoluminescence, thermal radiation, or stress energies. In contrast, transmission loss measurement cannot exclude these contributions. Figure 3(a) shows that the absorptivity calculated with Q_a is at most 3.5% smaller than that evaluated by the transmission loss measurement. This difference indicates that the contribution of photoluminescence, thermal radiation, and stress energies should be less than 3.5% of the incident light energy.

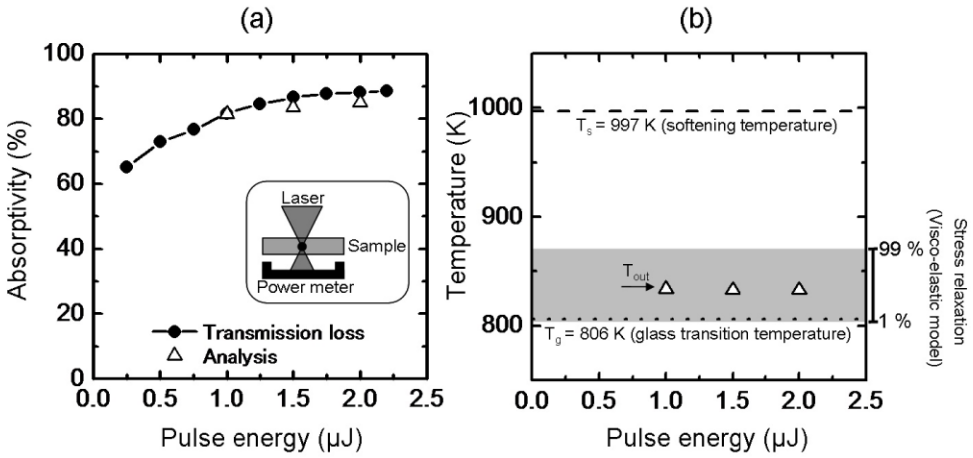

Fig. 3. (a) Optical absorptivity determined by the analysis and transmission loss measurement. (b) Comparison between the determined characteristic temperature (T_{out}) and other important transformation temperatures. The gray band indicates the temperature range where the estimated percentage of stress relaxation after 1-s laser irradiation changed from 1% to 99%.

The determined characteristic temperature thresholds (T_{out}) are shown in Fig. 3(b). The gray band indicates the temperature range where the estimated percentage of the stress relaxation after 1-s laser irradiation changed from 1% to 99%. This means that stress relaxation is almost complete when the temperature reaches above the gray band during the exposure time (= 1 s). The stress relaxation is estimated by the Vogt-Kelvin model, which is the basic model for the visco-elastic deformation (see ref. 9 for details). The T_{out} values for

#157072 - $15.00 USD
Received 26 Oct 2011; accepted 15 Nov 2011; published 4 Jan 2012

three pulse energies are located in the gray band. This indicates that, inside the outer boundary, visco-elastic stress relaxation had occurred during the exposure time. In contrast, outside the outer boundary, visco-elastic relaxation had not started during the exposure time. Therefore, the material outside of the boundary served as a wall for the materials inside the boundary. As the result, a clear boundary appeared.

Having determined the absorbed energy of one pulse, we evaluated the detailed temperature distribution with the absorbed energy fixed. Although we assumed an elliptically symmetric heat distribution to obtain the optical absorptivity and characteristic temperature, the actual heat distribution should be asymmetric in the beam propagation direction because of plasma dispersion and the Kerr effect [20]. In order to obtain a more plausible temperature distribution, we changed the shape of heat distribution only in the z direction to reproduce the entire shape of the outer boundary with the absorbed energy for one pulse fixed. We show the optical microscope image and the three-dimensional temperature distributions determined for 2.0 μJ in Figs. 4(a)–(d).

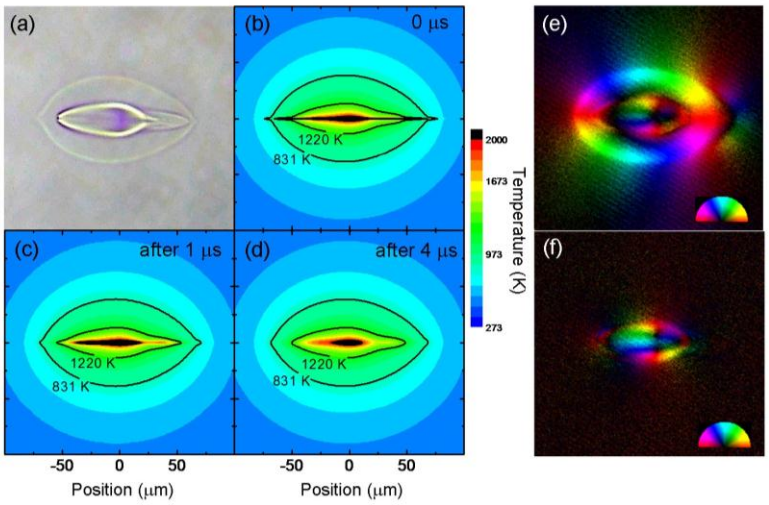

Fig. 4. (a) Optical microscope image and (b)–(d) three-dimensional temperature distributions under a pulse energy of 2.0 μJ at an ambient temperature of 298 K. (b) Just after final pulse irradiation. (c) 1 μs after final pulse irradiation. (d) 4 μs after final pulse irradiation. (e) Residual strain distribution after laser irradiation (f) Residual strain distribution after heat treatment. In (e) and (f), the brightness indicates the relative intensity of birefringence. The colors express the direction of the slow axis of the index ellipsoid. The direction corresponds to that in the inset of semicircular shape. The scale for each figure is identical to that in (c) and (d).

Figures 4(b), (c), and (d) show the temperature distributions at 0, 1, and 4 μs, respectively, after 1-s irradiation at 2.0 μJ of pulse energy, with the contour lines of the characteristic temperatures of the outer and inner boundaries drawn in the figures. The sharp edge near the beam propagation axis in the contour lines of T_{out} at 0 μs disappears after 1 μs owing to thermal diffusion, and the difference between 1 and 4 μs is small. Such cycles were repeated every 4 μs until the exposure of laser pulses was stopped. In contrast, such a sharp edge is not observed in the optical microscope image. This difference implies that the modification is slow enough that the sharp edge of the temperature distribution cannot affect the modification

Miyamoto et al. [4] proposed that in Schott D263 glass, the characteristic temperature of the outer boundary (T_{out}) is 1324 K and that of the inner boundary (T_{in}) is 3873 K. The estimated T_{out} in our analysis is much lower than their value, although the glass transition temperature (T_g = 830 K) and the softening temperature (T_s = 1009 K) of D263 [14] are close to those (T_g = 806 K and T_s = 997 K) of B270 [14]. The difference in T_{out} could be because of an invalid assumption in their analysis. They assumed T_{out} to be the glass-forming temperature

#157072 - $15.00 USD
Received 26 Oct 2011; accepted 15 Nov 2011; published 4 Jan 2012

(at a viscosity of 4.0 dPas) because welding between two glass plates occurs inside the outer boundary. However, there is no evidence that welding does not occur below this temperature. In addition, the difference between T_{out} and T_{in} in our analysis is smaller than their value. This is because we consider the temperature dependence of the specific heat. In our results, T_{in} is 1220 K, which is close to the glass-forming temperature (= 1306 K, viscosity of 4.0 dPas) of B270. To investigate the mechanism of inner boundary formation, we heat-treated the glass sample at T_g (= 806 K) for 1 h after laser irradiation. In Figs. 4(e) and (f), we show the residual strain distribution before and after the heat treatment, measured by using a polarization microscope with a liquid crystal compensator [21]. Before the heat treatment, the direction of the slow axis in Fig. 4(d) indicates that the strain was directed in the radial direction in the outer-modified region. This implies that the outer-modified region is compressed owing to thermal expansion in the central high-temperature region during laser exposure. After the heat treatment, as is shown in Fig. 4(f), the strain in the inner-modified region still remained, whereas that in the outer modified region disappeared. Given that the strain cannot be removed by heat treatment at T_g, formation of the inner-modified region is likely to include the flow of glass elements [15]. In addition, the changes cannot be reversed to the original state unless the temperature of the heat-treatment is so high that the elements in the glass can move freely. Blondin et al. suggested that the change in the refractive index distribution near the focal spot under high-repetition fs laser irradiation is likely related to the flow of glass elements [11]. Our experimental result supports their suggestion.

6. Conclusion

In conclusion, we determined three-dimensional temperature distributions and considered the modification mechanism in a glass exposed to laser irradiation. The optical absorptivity evaluated with the temperature distribution is approximately 80% and at most 3.5% smaller than that evaluated by the transmission loss measurement. Based on the temperature distribution and the strain distribution, we conclude that the formation of the outer-modified region is due to visco-elastic deformation, and that of the inner-modified region is due to the flow of glass elements.

Acknowledgments

The authors thank Dr. Nishi and Mr. Iwahara at Kyoto University for fruitful discussions. This work was supported by a Grant-in-Aid for JSPS Fellows.

#157072 - $15.00 USD Received 26 Oct 2011; accepted 15 Nov 2011; published 4 Jan 2012